



Effect of Sinusoidal Corrugated Bed on Hydraulic Jump Characteristics in Dense Flows

Seyed Reza Mousavi¹, Amir Hossein Parand², Nader Barahmand³

1-Department Of Civil Engineering, Marvdasht Branch, Islamic Azad University, Marvdasht, Iran

2- Department Of Civil Engineering, Marvdasht Branch, Islamic Azad University, Marvdasht, Iran

Email: a_h_parand@yahoo.com

3-Department Of Civil Engineering, Larestan Branch, Islamic Azad University, Larestan, Iran

Abstract: Dense flows are caused by differences in density or volume mass of two fluid. Due to density difference between this flow and the environmental fluid on it, vortexes are formed in the interface between them that caused entering of environmental fluid into flow. So dense flow characteristics of environmental flow is differ from open channel normal flows. The aim of our research is investigation the effect of corrugated bed on dense flow hydraulic jump characteristics. The fluent software was used. For this investigation six kind of corrugated bed with different wave steepness (h/B) were used. Numerical results showed that RNG hydraulic models were more compatible with experimental results. Also hydraulic jump in dense flow observed in all of models. If the primary Froude number keep constant, the primary point of jump transferred to the upstream and the conjugate depths of hydraulic jump decrease by increasing bed wave steepness ratio.

Key words: The Dense Flow, Sinusoidal Corrugated Bed, Hydraulic Jump, Turbulence Model of RNG.

Introduction

Dense flows (having density) are from the category of the flows which are created due to the difference of the volume mass (density) between two fluids. The dense flow is one of the important mechanisms of transferring sediments in lakes, seas and oceans. In the field of hydraulic, we can name the downstream and upstream flows in the reservoirs of dams, motion of the solid sediments in the ponds, the salt water flow under the fresh water flow in estuaries as the dense flows. In nature, the dense flows occur in large scales and include the movement of the cool air by its flowing on the snow or cool land. Also, coldness progress under the warm air, the flow containing particles in the sea floor sediments, movement of avalanche and ground collapse due to the landslide are other examples of the dense flows.

The first field observations of the dense flows containing fine-grained material (turbid flows) were carried out in Geneva Lake in Switzerland. As it is shown in figure (1), the river fraught with Rhine sediment has entered Geneva Lake through a lower dense flow. Due to this flow, a channel of 200 meters width and 15 meters depth and 9 km length has been created in the lake (Garcia, 1992). The observations have indicated that even completely low densities (less than one gram per liter) can be enough for revealing the turbid flows in the field. Of course, the turbid flows created in the salty environments require higher densities of suspended sediments (about 35 to 40 grams per liter) (Mulder and Syvitsky, 1995).

Only in the recent 80 years, numerous numerical models have been created for the dense flows. These models have been often created regarding to the equations of continuity of mass and momentum for both phases of fluid and solid and also the diffusion equation (which indicates the balance between the changes rate of the suspended materials in the control volume and the rate of exit of sediment from the control volume). Of course, parameters like speed of the particles' falling or the sediment mixing coefficient and so on can make it difficult to solve the above equations. Also, since solving these equations are usually accompanied with hypotheses such as layered flow, permanence, existence of a particle in the flow, ignoring the effect of particles on each other and so on, therefore, it is possible that in some cases, the results of the numerical models are not significantly consistent with the real ones.

As time passed, various researchers have tried to minimize these errors and create more complete numerical models; here we will refer to some of them.

Stow and Bowen (1980) posed a simple model for the turbid flows with the power of deposition of the sediments.

Also, Farrell and Stephen (1988) presented a two dimensional model for the immersed density in the repositories with simple geometry. They utilized a $k - \varepsilon$ model in order to solve the equations.

Oehy and Schleiss (2001) investigated the deposited sediments caused by the existence of a barrier in the path of the turbid flow in three dimensional method.

Skene et al. (1997) used a model in order to simulate the constant flow and predicted the changes of the distribution of deposit of sediments due to topographic barriers.

Mahdi Zadeh and Firouz Abadi (2009) studied and compared the two-dimensional simulation of the dense flow with considering different kinds of turbulence. They used models of $k - \varepsilon$, V2-f and RNG, and it was observed that V2-f model was the best model of numerical simulation.

About the necessity of conducting this research, it should be noted that no study has been carried out related to the behavior of the dense flow in facing the sinusoidal-shaped bed of the channel. Therefore, in this study, we investigated the hydraulic jump on six different types of wavy contexts with the wave slope of (h/B).

Research Methodology

a) The equations ruling the flow field

Reynolds-averaged equations of the conservation of mass and momentum for a nonpermanent medium-density flow are as following:

$$1- \quad \frac{\partial \rho}{\partial t} + \frac{\partial(\rho U_i)}{\partial x_i} = 0$$

$$2- \quad \frac{\partial(\rho U_i)}{\partial t} + \frac{\partial(\rho U_i U_j)}{\partial x_j} = -\frac{\partial P_i}{\partial x_i} + \rho g'_i + \frac{\partial}{\partial x_j} \left(\mu \frac{\partial U_i}{\partial x_j} - \overline{\rho U_i U_j} \right)$$

U_i and U_j are the components of the Reynolds-averaged speed vector of the dense flow in the Descartes directions x_i and x_j ; t is time, p_i is the Reynolds-averaged pressure in the Descartes direction of x_i , ρ is the density of the dense fluid and μ is the dynamic viscosity of the fluid. Meanwhile, the Reynolds tensions of $-\overline{\rho U_i U_j}$ and the reduced gravity of g'_i are calculated as following. It is noteworthy that the Reynolds tensions have been obtained as following by using the Boussinesq theory.

$$3- \quad -\overline{\rho U_i U_j} = \mu_T \left(\frac{\partial U_i}{\partial x_j} + \mu \frac{\partial U_j}{\partial x_i} \right) - \frac{2}{3} \left(\rho K + \mu_T \frac{\partial U_i}{\partial x_i} \right) \delta_{ij}$$

$$4- \quad g'_i = g_i \frac{\rho - \rho_a}{\rho_a}$$

ρ_a is the environmental density of the fluid (here it is clean water), δ_{ij} is the Kronecker delta and K is the kinetic energy of turbulence. Moreover, g_i is the gravitational acceleration and for $i=1,2,3$, it equals to $(g \sin \theta, -g \cos \theta, 0)$. Also θ is the slope of channel's bed. μ_T is the viscosity of the vortex which is obtained from

a $K - \varepsilon$ model and from the equation of $\mu_T = \rho C_\mu \frac{K^2}{\varepsilon}$ in which ε is the dissipation rate of kinetic energy of turbulence and C_μ is the constant of the equation.

It should be mentioned that in addition to the above equations, the equation of conservation of mass of sediments (the soluble materials) in a nonpermanent dense flow is as following:

$$5- \frac{\partial(\rho C)}{\partial t} + \frac{\partial[(\rho U_j - v_s \delta_{j2})C]}{\partial x_j} = \frac{\partial \left[\left(\rho \lambda + \frac{\mu_r}{S_c} \right) \frac{\partial C}{\partial x_j} \right]}{\partial x_j}$$

In which λ is the diffusion coefficient of the fluid, v_s is the velocity of the sediment particles (for the soluble materials, it equals to zero) and δ_{j2} is a component of Kronecker delta in the opposite direction of the gravitational acceleration. Also S_c is the Schmidt number of turbulence. This number like Prandtl number is under the influence of floating. But in dense flows, its value is usually considered equal to the unit.

$$C = \frac{\rho - \rho_a}{\rho_s - \rho_a}$$

Also, $\rho_s - \rho_a$ is the Reynolds-Averaged density of sediments or salt in the dense fluid and ρ_s is the density of the suspended sediments or salt. In the momentum equation, it is considerable that the pressure P in the distance of y is obtained from the following equation:

$$6- \frac{P}{\rho_a} = \frac{P_0}{\rho_a} - g'(H - h) + \rho g \frac{(H - y)}{\rho_a}$$

In which P_0 is the pressure in the free surface of the environmental fluid and H is the total depth of the fluid with considering the thickness of the dense flow of h .

Finally, it should be noted that the turbulence models have great diversity. From these models, we can refer to the zero-equation model (such as Prandtl mixing length model, Baldwin and Lomax mixing length model and B.C and Smith mixing length model), the standard two equations model of $k-\varepsilon$, $k-\varepsilon$ model from the RNG type, $k-\varepsilon$ realizable model, $k-\varepsilon$ modified model, $k-\varepsilon$ model for the low Reynolds numbers, $k-\omega$ model, v^2-f model, RSM Reynolds stress equation model, Algebra stress model, RNG model, simulation of Large Scale vortices LES. In this study, $k-\varepsilon$ standard models, RNG $k-\varepsilon$ model, and $k-\varepsilon$ model existing in the Fluent software have been used for numerical simulation.

b) Modeling

The current study has been conducted by using Fluent Software. Withal, the tests of Garcia (1993) were used for the calibration of the numerical model with the fluid dynamic calculation Fluent software. The geometry of the experimental channel of Garcia (1993) was drawn by Gambit 2.4.6 software. Meshing was conducted by quadrilateral control volumes Map type. This type of meshing is from the kind of structured meshing. The boundary condition of pressure outlet was considered for the free surface of the environmental fluid and the exit place of the flow, the Wall boundary condition for the slide valve and the bed of channel and the Inlet velocity boundary condition was considered for the location under the slide valve. Velocity, volume concentration and thickness of the dense flow at the inlet (in the slide valve) were from the problem's data and were obtained from the data of Garcia (1993).

Results and Discussion

In this study, we used 7 types of wavy beds with the wave slope (h/B) equal to 0, 0.25, 0.5, 0.75, 1, 1.5, and 2. It must be mentioned that the wave slope which is equal to zero is in fact the indicator of the flat bed. Meanwhile, in this study, we used six values for the primary dense Froude number (0.3, 0.5, 1, 1.86, 3, and 5). The dense Froude number of 1.86 indicates the Sall29 test of Garcia (1993).

a) Calibration of the Model

A network with uniform dimensions of 500*14000 was used for meshing. As it is observed in figure (2), the calculative results have appropriate consistence with the laboratory results. Moreover, a large number of meshes exist in the corrugated area and this can model the effect of the corrugated bed on the dense flow.

b) Appropriate Turbulence Model

In this part of the study, we have used several turbulence models (the standard type of $k-\varepsilon$ model, RNG, Realizable and the standard $k-\omega$) in order to estimate the longitudinal profile of the dense flow of Sal29 test. Figure (3) illustrates the longitudinal profile of the dense flow for this test and also the implemented numerical models for this test. In addition, it should be stated that the height or thickness of the dense flow

have been calculated from the bed to the place in which the longitudinal velocity value of the dense flow is equal to zero.

As it is observed in figure (3), in the above test, jump has occurred in the distance of about 5.4 meters from the slide valve. In other words, jump has started in the horizontal part of the bed, it should be noted that just the $k-\varepsilon$ model from the kind of RNG has a start point like the test, but the jump in the other turbulence models like the $k-\varepsilon$ model from the standard type and Realizable model have occurred in the distance of 5 meters to the slide valve (just at the break point of the slope). Moreover, in the model of k-w, the jump has been transferred to upside and its length has decreased.

Therefore, $k-\varepsilon$ model from the RNG type is the most compatible one with the laboratory values.

After this model, models $k-\varepsilon$ from the Realizable, standard and finally the k-w model is very careless in this field. In the interim, all turbulence models have estimated the dense flow value a bit more than the real value; of course, in the $k-\varepsilon$ model from RNG type this difference in value is negligible and can be ignored.

c) Investigation of the impact of the wavy sinusoidal bed of channel on the characteristics of the dense flow

In all numerical models, the hydraulic jump was observed in the same dense flow and it was changing depending on the flow conditions (the primary Froude number in the slide valve location Frd_0) and the slope of the wave of the corrugated bed (h/B), the location of the occurrence of the hydraulic jump and also the conjugate depth ratios of the jump h_1/h_2 . In other words, even for the flows which had been critical or subcritical at the beginning, the flow has been immediately changed into supercritical and then, the hydraulic jump has occurred under the influence of the horizontal bed of the downside.

As it is seen in the figure (4), the location of the start point of the created hydraulic jump has been drawn in proportion to the primary Froude number Frd_0 .

According to this figure, in case of the constant primary Froude number, with the increase of the bed wave slope ratio, the start point of the jump is transferred to the upstream. In other words, the distance of the start point from the slide valve decreases so that in the primary Froude number equal to 0.3, with the increase in the wave slope h/B from zero to two, the location of the start point of jump changed from 5 m to 3.3 m from the slide valve and this indicated a difference about 34 percent. In other words, the change in the wave slope from zero to two has caused a 34 percent change in the primary location of the hydraulic jump.

That is to say that with increase in h/B ratio, the value of the secondary flows and the vortex on the corrugated bed have become more significant; and consequently the energy amortization has increased and this has led to the reduction of the certain force in a less distance from the slid valve (compared to the values less than h/B) and this is itself the reason of the occurrence of the hydraulic jump to upstream.

As it can be seen in the figure (5), the conjugate depths ratio of hydraulic jump h_1/h_2 has been drawn in proportion to the primary Froude number Frd_0 . It should be mentioned that the horizontal axis is the primary Froude number. Meanwhile, the vertical axis is the conjugate depths ratio of the hydraulic jump h_1/h_2 . Also it should be mentioned that thickness values of the dense flow in the start and finish points of the jump (respectively h_1 and h_2) have been determined in observational form and according to the graphical charts of Fluent software.

According to this figure, in case of the constant value of the primary Froude number, with increase in bed wave slope ratio, conjugate depths ratio of the hydraulic jump decrease. So that in the primary Froude number of 1.86, with increase in the wave slope of h/B from zero to two, the conjugate depths ratio changed from 2.26 to 1.55 and this indicates a difference about 31.4 percent. In other words, change in the wave slope from zero to two has caused a 31.4 percent change in conjugate depths ratio of the hydraulic jump.

Another reason is that with increase in the h/B ratio, the bed becomes rougher and the value of the secondary flows and the vortex on the wave bed become significant. Consequently, the energy amortization increases and this leads to the reduction of the certain force in the start point of jump and finally the reduction of the conjugate depths ratio.

Conclusion

By using the conducted numerical study, the following overall results were obtained:

1. A network with uniform dimensions of $500*14000$ had suitable compatibility with the experimental results.
2. Compared to the other models of turbulence, the turbulence model of $k-\varepsilon$ from the RNG type had more consistency with the experimental observations

3. All of the turbulence models have estimated the dense flow value a bit more than its real value; of course in the $k-\epsilon$ model from the RNG type, this difference in value is negligible and can be ignored.
4. In the whole numerical modeling, the hydraulic jump has been observed in the same dense flow.
5. In case of the constant primary Froude number, with increase in the wave slope ratio of the bed, the start point of jump is transferred to the upstream.
6. In case of the constant primary Froude number, with increase in the wave slope ratio of the bed, conjugate depths ratio of the hydraulic jump decreases.

References

1. Berhamand, N.; Mousavi, R., 2013, Comparing the Different Similar of Turbulence in Order for Appropriate Simulation of the Dense Streams in the Vicinity of the Location of the Reduction of the Bed Slope. *Water Engineering Magazine*, the sixth year, No. 16
2. Farrel. GJ, Stefan H. 1988. Mathematical modeling of plunging reservoir flows. *J. Hydraul. Res.*, 26(5), 525–537.
3. Garcia, M.H. 1992. Turbidity currents. *Encyclopedia of earth systems science*, Vol. 4, Academic Press, San Diego, Calif., 399-408.
4. Garcia, M.H. 1993. Hydraulic jumps in sediment-driven bottom currents. *J. Hydraul. Eng.*, 119(10), 1094-1117.
5. Mulder, T., and Syvitsky, J. P. M. 1995. Turbidity currents generated at river mouths during exceptional discharges to the world oceans. *J. Geology.*, 103, 285–299.
6. Mehdizadeh, A., Firoozabadi, B. 2009. Simulation of a Density Current Turbulent Flow Employing Different RANS Models: A Comparison Study. *Scientia Iranica, Transaction B: Mechanical Engineering*. 16(1), 53-63.
7. Oehy, Ch., and Schleiss, A. 2001. Numerical modeling of a turbidity current passing over an obstacle—Practical application in Lake Grimsel, Switzerland. *Proc., Int. Symp. On Env. Hydr. (CD-ROM)*, Tempe, Ariz.
8. Skene, K. I., Mulder, T., Syvitski, J. P. M. 1997. INFLO1: a model predicting the behaviour of turbidity currents generated at river mouths. *Comput. Geosci.* 23, 975– 991.
9. Stow D. A., and Bowen, A. J. 1980. A physical model for the transport and sorting of fine-grained sediment by turbidity currents. *Sedimentology*. 27, 31–46.

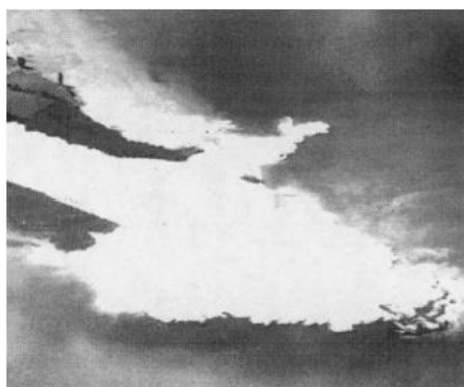


Figure (1): the inlet turbid flow to Geneva Lake through Rhine River (Garcia, 1992)

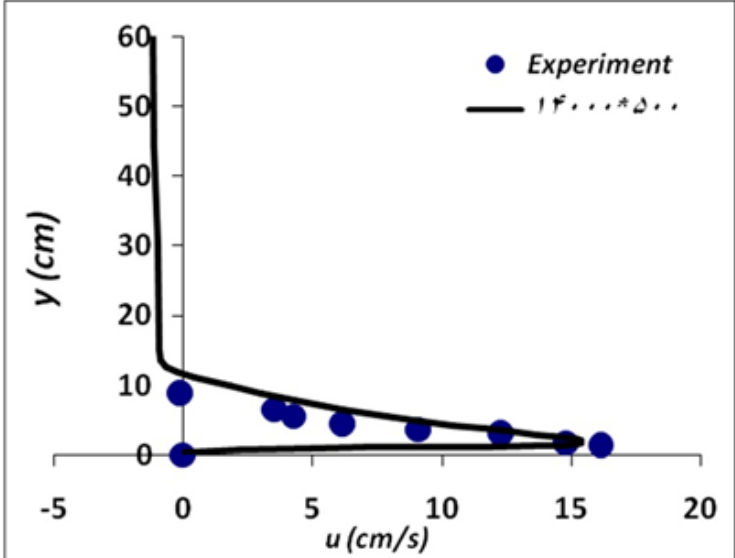


Figure (2): the velocity profile for numerical modeling of Sall29 test

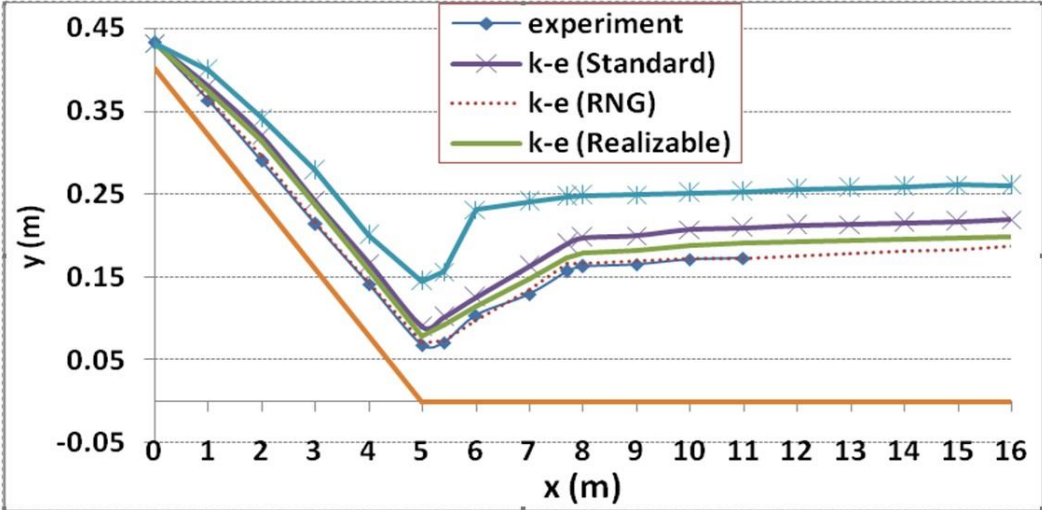


Figure (3): the longitudinal profile of the dense flow for Sall29 test and the numerical models related to this experiment with different models of turbulence and according to the natural bed

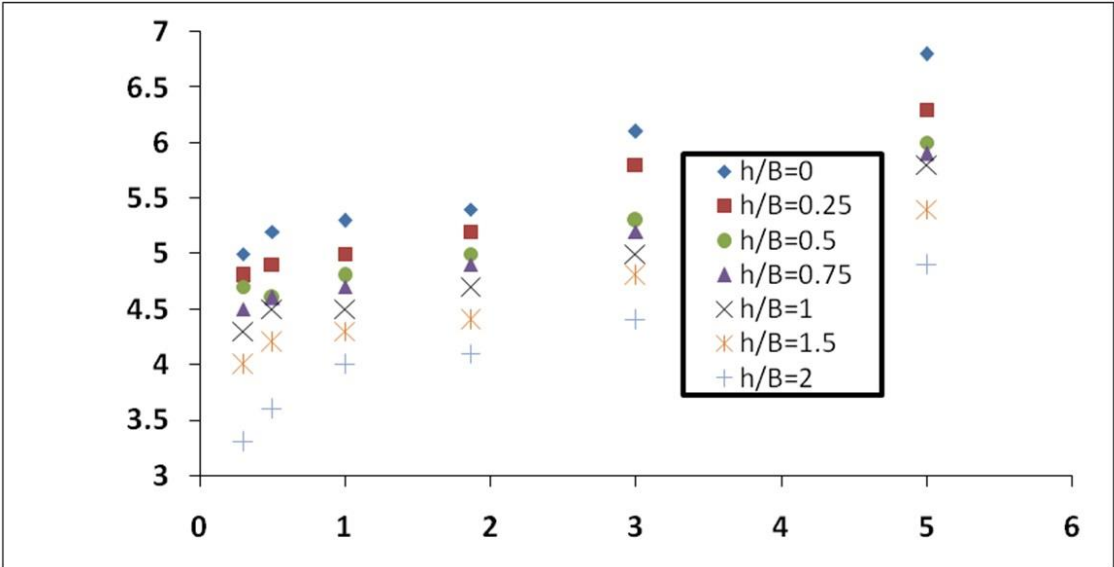


Figure (4): changes of the start point location of the hydraulic jump (vertical axis) regarding to the changes of the primary Froude number Fr_{d0} (horizontal axis)

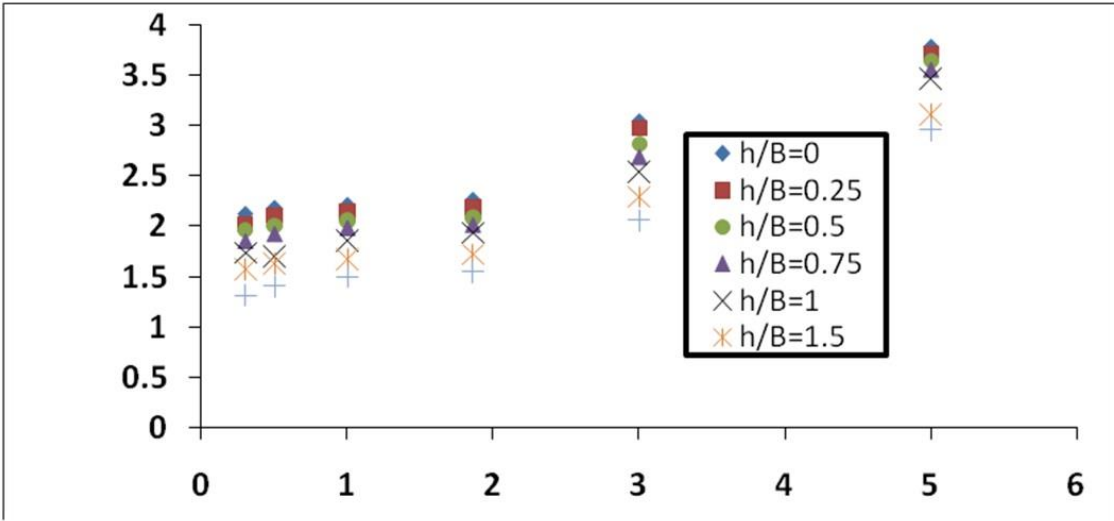


Figure (5): changes of the conjugate depths ratio of the hydraulic jump (vertical axis) regarding to the changes of the primary Froude number Fr_{d0} (horizontal axis)